

Single tellurium whisker for the NO₂ gas sensor: synthesis and rapid demonstration of sensitivity

© M.R. Rabadanov¹, V.V. Krivetskiy², A.M. Ismailov¹, M.A. Umakhanov¹, M.Kh. Rabadanov¹

¹Dagestan State University, Makhachkala, Dagestan Republic, Russia

²Moscow State University, Moscow, Russia

E-mail: egdada@mail.ru

Received August 15, 2025

Revised September 2, 2025

Accepted September 3, 2025

We report a method for synthesizing tellurium (Te) whiskers, both solid and hollow, with reproducible morphology and geometry. The approach based on tellurium evaporation in a hydrogen atmosphere enables precise control over whisker characteristics through the adjustment of key process parameters: crucible temperature, substrate temperature, their temperature gradient, and hydrogen pressure. The paper demonstrates the possibility of direct integration of an individual Te whisker into a micro-sensor structure and presents the results of rapid evaluation of room-temperature NO₂ sensing for whiskers of two diameters (28 and 60 μm). At the concentration of 5 ppm, the sensor achieves sensitivity $S \approx 10\%$, while the minimum detected concentration is 0.3 ppm for the 28 μm whisker. The device exhibits a reproducible and reversible response highlighting its potential for application in miniature low-power gas analyzers.

Keywords: tellurium whiskers, gas sensors, nitrogen dioxide (NO₂), sensor response.

DOI: 10.61011/TPL.2026.01.62821.20474

In recent years, there has been growing interest in creating highly sensitive, selective and energy-efficient gas sensors (detectors) capable of operating at room temperature, which are important for portable environmental monitoring systems, industrial control and non-invasive medical diagnostics [1,2]. To achieve acceptable reaction kinetics, conventional sensors based on oxides (ZnO, SnO₂, WO₃, etc.) need heating to temperatures of 200–400 °C [3]. This not only increases the power consumption, but also gives rise to challenges concerning long-term stability because of thermal degradation and growth of grains in the sensitive layer. Tellurium, which is a *p*-type semimetal-semiconductor with a narrow band gap of ~ 0.35 eV, turned out to be one of the few materials that can detect a wide range of toxic gases (NO₂, NH₃, H₂S, Cl₂, CO, etc.) without heating the sensing element [4–14]. This opens the way for creating portable, wearable and autonomous sensor systems with ultra-low power consumption, which are able to operate for a long time being fed from miniature power supplies [15].

Earlier studies were devoted to tellurium films exhibiting at room temperature stable variations in resistance under the impact of oxidizing (NO₂, Cl₂) and reducing (NH₃, H₂S) gases [4–6]. Further studies have shown that the transition from continuous tellurium films to low-dimensional structures (whiskers and nanotubes [7–14], nanoparticles [16], 2D-tellurium (tellurene) [17]) significantly increases the material's specific surface area, enhances the effect of surface charge states and, thereby, increases sensor sensitivity by reducing their detection threshold.

Despite the efficiency of conventional methods for synthesizing Te whiskers, such as hydrothermal and solvothermal synthesis, physical vapor deposition, electrodeposition, and

also dissolution and recrystallization methods, has been extensively proven [18], their capabilities for ensuring precise control of morphology and high reproducibility have already been largely exhausted. This limitation stimulates the search for and development of alternative technological approaches capable of ensuring stable synthesis of Te whiskers with precisely specified structural and dimensional characteristics. Insufficient control of morphology and reproducibility, which is inherent in conventional synthesis methods, is a key factor limiting comprehensive and systematic investigation of performance characteristics of the Te-whisker-based gas sensors. In this regard, the main goal of this work was to develop a new synthesis method, namely, tellurium vapor transfer in a hydrogen environment. The method provides obtaining a Te whisker array with a preset and reproducible morphology. The paper presents the results of direct integration of a single Te whisker into the measuring microstructure as well as rapid assessment of its room-temperature gas-sensitive properties.

In this work, high-purity tellurium 6N (99.9999%) (5N Plus, Canada) was used. The Te whiskers were obtained by thermal-vacuum tellurium evaporation in hydrogen [19]. The method for obtaining Te whiskers involves controlling the crystallization process by monitoring the crucible zone temperature T_2 and substrate temperature T_1 , difference between them $\Delta T = T_2 - T_1$, and initial hydrogen pressure $P(\text{H}_2)$ in the reactor. The Te whisker morphology, as well as geometric dimensions, was examined with scanning electron microscope (SEM) Leo 1450 (Carl Zeiss, Germany) in the secondary-electron mode. The Te whisker crystalline structure was studied using diffractometer Empyrean Series 2 (PANalytical, Netherlands) based on

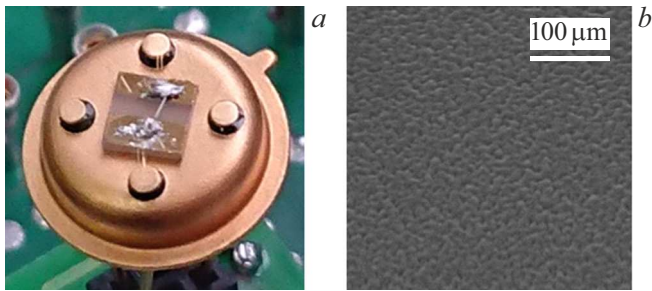


Figure 1. *a* — a photo of the experimental sample of the sensor structure; *b* — SEM image of the Te whisker side surface.

the $\text{CuK}\alpha$ radiation ($\lambda = 0.15406 \text{ nm}$). As the substrate, a micromesh was used (nichrome, filament diameter of $25 \mu\text{m}$, mesh size of $25 \times 25 \mu\text{m}$). Whiskers $10\text{--}100 \mu\text{m}$ in diameter were manipulated and transferred in the optical microscope field of view with a microwire.

For sensor measurements, we selected from the array two Te whiskers obtained under the following conditions: $T_2 = 600^\circ\text{C}$, $T_1 = 430^\circ\text{C}$, $\Delta T = 170^\circ\text{C}$, $P(\text{H}_2) = 0.8 \text{ atm}$. The samples are designated as follows: sample 1 is the Te whisker $28 \mu\text{m}$ in diameter, sample 2 is the Te whisker $60 \mu\text{m}$ in diameter. Fig. 1 presents a photo of a gas sensor sample assembled for investigation on the basis of casing KYuYaL.431433.018-03 (JSC Mars, Russia). In the center of the casing, a square substrate made of polycor ($3 \times 3 \times 0.5 \text{ mm}$) is fixed; on its surface, two parallel golden strips serving as contact pads are formed by magnetron sputtering. Between the pads there is a single tellurium whisker (sensitive element) attached to the golden strips with low-temperature Rose-type alloy, which prevents thermal damage (oxidation) of the Te crystal. To integrate the sample into the measuring system, each golden pad is connected to the corresponding casing terminal with two parallel golden wires $\sim 25 \mu\text{m}$ in diameter attached by ultrasonic microwelding.

The relative sensor response was defined as $S = (R_0 - R_g)/R_0$, where R_0 is the baseline resistance in air, R_g is the minimum resistance under gas exposure (NO_2). The response and recovery times were assumed to be time intervals during which the sensor electrical resistance reached 90% of R_0 and R_g , respectively. The detected gas concentration (in ppm) decreased stepwise: $5 \rightarrow 2.5 \rightarrow 1.25 \rightarrow 0.7 \rightarrow 0.3 \rightarrow 0$. Each level was set by a series of short gas–air pulses in the form of which the gas chamber was purged for 900 s with a 100-ml/min dry air flow to which gas at a preset concentration was admixed; after that, the chamber was purged with clean dry air during the same time period. The flows of air and gas to be mixed were set with high-precision mass flowrate controllers Bronkhorst (Netherlands). As the pure air source, pure air generator GChV 1.2 (LLC „Himelektronika“, Russia) was used. As the gas source, there was used a cylinder with the calibration gas mixture (LLC „Monitoring“, Russia).

The growth technique allows for wide-range control of the system supersaturation by varying process parameters (T_1 , T_2 , ΔT , $P(\text{H}_2)$) and thus for selecting the optimal modes for synthesizing Te whiskers of different size and morphology (solid/hollow). Fig. 2 presents the morphologies characteristic of tellurium whiskers: solid whisker (*a*) and hollow whisker in the form of a microtube (*b*). The array of whiskers always exhibits a spread in sizes, mainly in diameter, which is associated with local inhomogeneity of the substrate. No distinct boundary (in terms of process parameters) has been revealed between solid and hollow whiskers. Only modes in which structures of different morphological types predominate have been established. The Te whisker typical sizes are: diameter of $50 \text{ nm--}100 \mu\text{m}$, length up to 1.5 cm, growth rate of $200 \mu\text{m}/\text{min}$ ($\sim 1.2 \text{ cm}/\text{h}$), microtube wall thickness of $1\text{--}5 \mu\text{m}$. Fig. 1, *b* demonstrates a developed microrelief of the Te whisker surface. By varying the above-mentioned parameters, the relief may be intentionally modified so as to improve the sensory characteristics.

A sample for X-ray phase analysis was created from an array of parallel-oriented Te whiskers ($d = 10\text{--}80 \mu\text{m}$, $L \approx 8 \text{ mm}$) on a glass substrate; the beam was directed along the crystal axis, no sample rotation was performed. In this geometry, reflections (100), (200), (300) were recorded, as well as reflections from plane (110) and (220) arising because of random whisker rotation about the c axis (Fig. 3). Small half-width of main peak (100) FWHM $\approx 0.042^\circ$ (2θ) indicates high crystalline quality (superior to that of Te single crystals and epitaxial films) [20].

While the gas to be detected is bled in, dynamics of the resistance of two sensor samples made of single Te whiskers of different diameters demonstrates the expected characteristic response (Fig. 4, *a*). Initial resistance R_0 of sample 1 (a whisker of a smaller diameter) is $\sim 10.3 \text{ k}\Omega$, while that of sample 2 (a whisker of a larger diameter) is $\sim 4.5 \text{ k}\Omega$; this confirms the inverse R_0 dependence on the whisker diameter. In each case of pulsed introduction of NO_2 , resistance decreases because the adsorbed NO_2 molecule captures a Te valence electron, and concentration of holes increases. The response peaks at the same NO_2 concentration repeat with the same shape

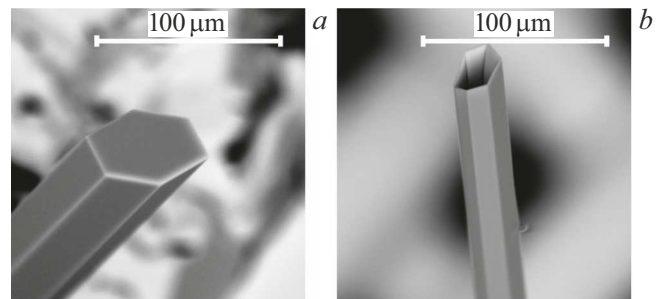


Figure 2. Morphology of Te whiskers. *a* — solid whisker; *b* — hollow whisker (microtube).

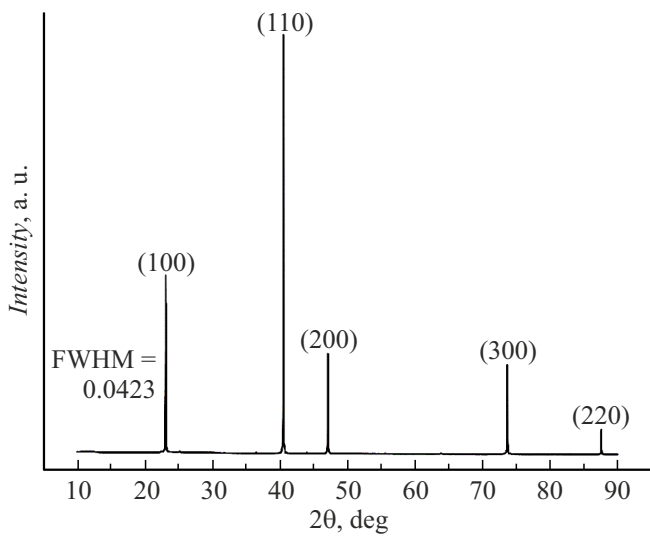


Figure 3. X-ray pattern of the Te whisker array.

and height, which demonstrates high reproducibility of adsorption-desorption processes. At the beginning of the experiment, a slight decrease in R_0 is observed, which is probably associated with thermal stabilization; when concentrations become lower, a moderate increase in the baseline is detected, which may be attributed to gradual surface passivation or accumulation of oxygen-containing radicals. Despite the difference in absolute values of R_0 , relative sensitivities $S = \Delta R/R_0$ of both samples do not differ significantly (Fig. 4, *b*). In the low concentration range of 0.3–0.7 ppm, the response of sample 2 is slightly higher. In the range of 1.25–2.5 ppm, the curves almost fully converge; at high concentrations of ~ 5 ppm, the predominance shifts to sample 1. Both dependences are close to quasi-linear, however, within

the range of 1.25–5 ppm sample 2 exhibits a more pronounced „saturation“, while the thin sample still exhibits a steeper increase. The minor predominance of thick whiskers at the minimal concentrations may be caused by differences in the defect structure, contacts, or statistics of active adsorption centers; this requires separate verification.

The response and recovery times of the sensors are presented in the Table.

Sensors based on single Te whiskers exhibit a relatively fast, stable and reversible response for devices operating without additional heating, since the response times of both samples do not exceed 10 min at the majority of concentration values. At the same time, small relative error indicates the signal stability, while recovery times ranging within 15 min confirm the signal reversibility.

Thus, a reproducible procedure for synthesizing Te whiskers with controlled morphology, dimensions, and surface nanostructure has been developed. Further research in this area will be aimed at improving the Te whisker synthesis procedure in order to overcome the key restrictions to the material as a sensor, namely, at reducing the long signal-recovery time, increasing stability of characteristics under the condition of variable humidity, and increasing the selectivity (distinguishing gases within the same class). The most promising approach seems to be using as a sensor element the hollow Te whiskers (microtubes) (Fig. 2, *b*). The advantage of Te microtubes is that their surface/volume ratio is higher than that of solid whiskers, which provides a larger specific surface area for the detected gas adsorption/desorption.

Conflict of interests

The authors declare that they have no conflict of interests.

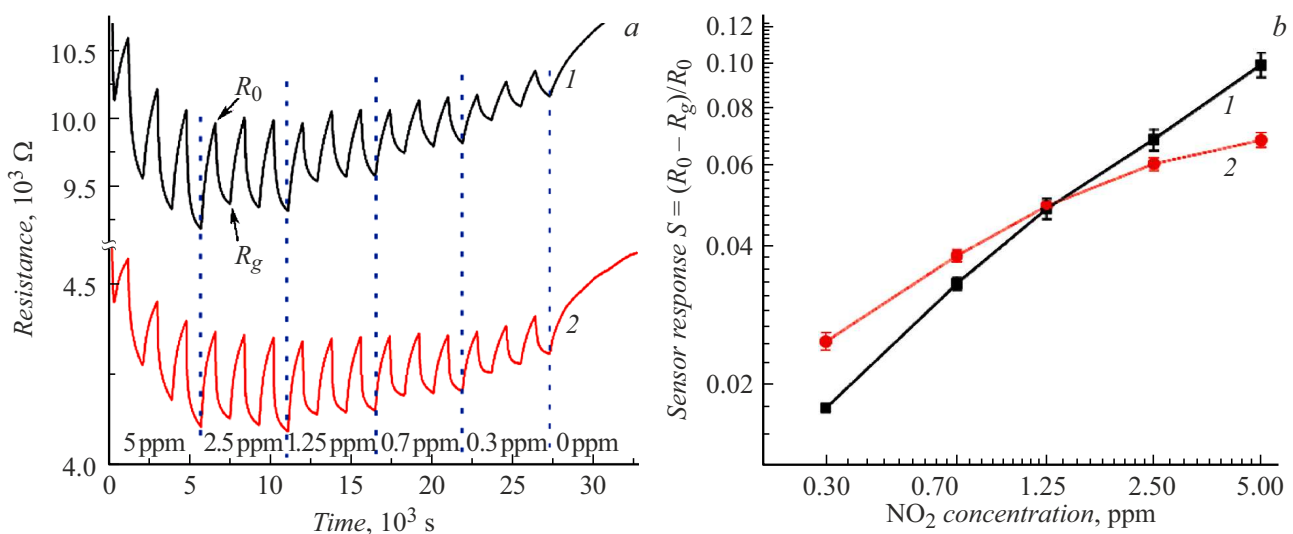


Figure 4. *a* — time dependences of the gas sensor resistance; *b* — relative sensor response S versus NO_2 concentration for gas sensors. The curves are numbered according to the sample numbers.

Response and recovery times of sensors based on hollow Te whiskers

Concentration of NO ₂ , ppm	Sample 1		Sample 2	
	Response time, s	Recovery time, s	Response time, s	Recovery time, s
5	521	683	576	613
2.5	493	756	402	702
1.25	548	779	338	729
0.7	612	791	385	742
0.3	646	825	371	783

References

- [1] L.-X. Ou, M.-Y. Liu, L.-Y. Zhu, D.W. Zhang, H.-L. Lu, *Nano-Micro Lett.*, **14**, 206 (2022). DOI: 10.1007/s40820-022-00956-9
- [2] B. Zong, S. Wu, Y. Yang, Q. Li, T. Tao, S. Mao, *Nano-Micro Lett.*, **17**, 54 (2025). DOI: 10.1007/s40820-024-01543-w
- [3] A. Dey, *Mater. Sci. Eng. B*, **229**, 206 (2018). DOI: 10.1016/j.mseb.2017.12.036
- [4] S. Sen, K.P. Muthe, N. Joshi, S.C. Gadkari, S.K. Gupta, Jagannath, M. Roy, S.K. Deshpande, J.V. Yakhmi, *Sensors Actuators B*, **98** (2-3), 154 (2004). DOI: 10.1016/j.snb.2003.10.004
- [5] D. Tsiulyanu, A. Tsiulyanu, H.D. Liess, I. Eisele, *Thin Solid Films*, **485** (1-2), 252 (2005). DOI: 10.1016/j.tsf.2005.03.045
- [6] T. Siciliano, M. Di Giulio, M. Tepore, E. Filippo, G. Micocci, A. Tepore, *Sensors Actuators B*, **135** (1), 250 (2008). DOI: 10.1016/j.snb.2008.08.018
- [7] D. Tsiulyanu, *Beilstein J. Nanotechnol.*, **11**, 1010 (2020). DOI: 10.3762/bjnano.11.85
- [8] S. Sen, M. Sharma, V. Kumar, K.P. Muthe, P.V. Satyam, U.M. Bhatta, M. Roy, N.K. Gaur, S.K. Gupta, J.V. Yakhmi, *Talanta*, **77** (5), 1567 (2009). DOI: 10.1016/j.talanta.2008.09.055
- [9] T. Siciliano, E. Filippo, A. Genga, G. Micocci, M. Siciliano, A. Tepore, *Sensors Actuators B*, **142**, 185 (2009). DOI: 10.1016/j.snb.2009.07.050
- [10] Z. Wang, L. Wang, J. Huang, H. Wang, L. Pan, X. Wei, *J. Mater. Chem.*, **20** (12), 2457 (2010). DOI: 10.1039/b924462j
- [11] Y.C. Her, S.L. Huang, *Nanotechnology*, **24** (21), 215603 (2013). DOI: 10.1088/0957-4484/24/21/215603
- [12] H. So, J. Yoo, K. Ryu, M.H. Yang, K.J. Lee, *Ceram. Int.*, **45** (6), 7226 (2019). DOI: 10.1016/j.ceramint.2019.01.003
- [13] T. Siciliano, A. Genga, G. Micocci, M. Siciliano, M. Tepore, A. Tepore, *Sensors Actuators B*, **201**, 138 (2014). DOI: 10.1016/j.snb.2014.04.098
- [14] L. Guan, S. Wang, W. Gu, J. Zhuang, H. Jin, W. Zhang, T. Zhang, J. Wang, *Sensors Actuators B*, **196**, 321 (2014). DOI: 10.1016/j.snb.2014.02.014
- [15] L. Wang, X. Yao, Y. Zhang, G. Luo, B. Wang, X. Yu, *Next Mater.*, **2**, 100092 (2024). DOI: 10.1016/j.nxmater.2023.100092
- [16] S. Yoon, T. Kim, S.-S. Chee, Y. Kim, H. Jung, *Appl. Surf. Sci.*, **684**, 161800 (2025). DOI: 10.1016/j.apsusc.2024.161800
- [17] Y. Je, S.S. Chee, *Electron. Mater. Lett.*, **21** (1), 94 (2025). DOI: 10.1007/s13391-024-00520-0
- [18] H. Zhu, L. Fan, K. Wang, H. Liu, J. Zhang, S. Yan, *Nanomaterials*, **13**, 2057 (2023). DOI: 10.3390/nano13142057
- [19] A.M. Ismailov, I.M. Shapiev, M.Kh. Rabadanov, I.Sh. Aliev, *Tech. Phys. Lett.*, **41** (1), 83 (2015). DOI: 10.1134/S1063785015010265.
- [20] M.R. Rabadanov, A.A. Stepurenko, A.E. Gummetov, A.M. Ismailov, *Semiconductors*, **55**, 551 (2021). DOI: 10.1134/S1063782621060129.

Translated by EgoTranslating